

Inflation models selected by the swampland distance conjecture with the Lyth bound

Yuma S. Furuta^{1,2}, Yuta Hamada^{1,2} and Kazunori Kohri^{3,4,2,5}

¹ *School of High Energy Accelerator Science,
Graduate University for Advanced Studies (SOKENDAI),
1-1 Oho, Tsukuba, Ibaraki 305-0801, Japan*

² *Theory Center, IPNS, High Energy Accelerator Research Organization (KEK),
1-1 Oho, Tsukuba, Ibaraki 305-0801, Japan*

³ *Division of Science, National Astronomical Observatory of Japan,
2-21-1 Osawa, Mitaka, Tokyo 181-8588, Japan*

⁴ *School of Physical Sciences, Graduate University for Advanced Studies (SOKENDAI),
2-21-1 Osawa, Mitaka, Tokyo 181-8588, Japan and*

⁵ *Kavli IPMU (WPI), UTIAS, The University of Tokyo, Kashiwa, Chiba 277-8583, Japan*

(Dated: August 4, 2025)

Abstract

We investigate the extent to which the Swampland Conjecture can be employed to constrain large-field inflationary models from the perspective of quantum gravity consistency. In particular, we focus on the Swampland Distance Conjecture, which imposes an upper bound on the amplitude of primordial gravitational waves predicted by large-field inflation scenarios. This provides a striking contrast with the well-known Lyth bound, which yields a lower bound on the tensor-to-scalar ratio in such models. The two bounds thus play complementary roles in assessing the viability of inflationary scenarios. We demonstrate that, for certain representative large-field inflation models, the Swampland Distance Conjecture alone can impose more stringent upper limits on the tensor-to-scalar ratio than current observational constraints from the cosmic microwave background. These findings highlight the utility of Swampland criteria as a theoretical discriminator among competing inflationary models, independent of empirical data.

I. INTRODUCTION

Cosmic inflation offers elegant resolutions to several fundamental problems in standard cosmology, including the horizon problem, the flatness problem, the monopole problem, and the origin of primordial density perturbations [1]. As such, uncovering the underlying mechanism responsible for inflation remains one of the most pressing and central challenges in modern theoretical cosmology. Despite its theoretical success, the precise nature of the scalar field ϕ , commonly referred to as the inflaton field that is believed to have driven inflationary dynamics has yet to be established. Neither the energy scale at which inflation occurred nor its precise epoch in cosmic history has been directly probed by current observational data. Observations of the cosmic microwave background (CMB), particularly its temperature anisotropies and polarization patterns, have so far yielded only upper bounds on the inflationary energy scale, constraining it to be below approximately 10^{16} GeV. This constraint is typically expressed in terms of the tensor-to-scalar ratio r , with the most stringent current bound being $r < 0.036$ [2, 3].

On the theoretical front, there exist complementary efforts to constrain the energy scale of inflation based on internal consistency relations derived from purely theoretic arguments. One such relation is the Lyth bound, which applies to slowroll models with super-Planckian field excursions, and provides a model-independent lower limit on r . However, even when considering both observational upper bounds and theoretical lower bounds, significant uncertainties remain regarding the model-dependent functional form of the inflaton potential $V(\phi)$ and the total field excursion $\Delta\phi$ during inflation.

Furthermore, recent developments in quantum gravity, particularly in the context of string theory, have motivated theoretical constraints on effective field theories via the so-called Swampland Conjectures [4]. In particular, the Swampland Distance Conjecture (SDC) [5] posits that effective field theories with trans-Planckian field excursions are incompatible with a consistent UV-completion in quantum gravity. The SDC, if valid, would place nontrivial theoretical constraints on inflationary model building, potentially ruling out large classes of models otherwise consistent with observations.

In this work, we present a detailed calculation of the tensor-to-scalar ratio as a function of $\Delta\phi$ for several representative large-field inflation models. Under specific assumptions, we demonstrate that the Swampland Distance Conjecture can, in certain cases, impose more

stringent bounds than those derived from current observational data.

The structure of the paper is as follows: In Section II, we review the Swampland Conjecture and its implications for inflationary dynamics. Section III outlines the Lyth bound. In Section IV, we introduce a selection of concrete large-field inflation models. Section V presents detailed model-dependent predictions for the tensor-to-scalar ratio and discusses the interplay between observational constraints and theoretical bounds. We summarize our findings and conclude in Section VI. Throughout this paper, we adopt natural units where $\hbar = c = 1$.

II. BOUND FROM THE SWAMPLAND DISTANCE CONJECTURE

By using SDC, the authors in [6] argues that the Hubble expansion rate during the primordial inflation should be smaller than the cutoff scale, $H \leq m_{\text{pl}} e^{-\lambda_{\text{dc}} \Delta\phi / m_{\text{pl}}}$. Here λ_{dc} is the exponential rate at which an infinite tower of states becomes light, m_{pl} is the (reduced) Planck mass ($\simeq 2.4 \times 10^{18}$ GeV), and $\Delta\phi$ is the excursion distance of the inflaton ϕ during the inflation. The constraint can be viewed as the upper bound on the field excursion [6]

$$\frac{\Delta\phi}{m_{\text{pl}}} \leq \frac{1}{\lambda_{\text{dc}}} \log \left(\frac{m_{\text{pl}}}{H} \right). \quad (1)$$

When we rewrite this inequality as a relation between $\Delta\phi$ and the tensor-to-scalar ratio r , we obtain

$$\frac{\Delta\phi}{m_{\text{pl}}} \leq \frac{1}{2\lambda_{\text{dc}}} \log \left(\frac{2}{\pi^2 A_s r} \right), \quad (2)$$

where A_s is the amplitude of the curvature perturbation ($\sim 2.1 \times 10^{-10}$) produced by the inflation at the horizon crossing of a large scale (e.g., $\sim 0.05 \text{Mpc}^{-1}$) [7]. Based on the emergent string conjecture [8], the sharpened distance conjecture [9, 10] (see also [11]) puts lower bound on the parameter λ_{dc} to be $\lambda_{\text{dc}} \geq \frac{1}{\sqrt{d-2}}$, where d is the number of dimensions. For a concrete values of λ_{dc} , the following three are chosen in this paper.

$$\lambda_{\text{dc}} = \begin{cases} 1 & \text{(a reference value),} \\ \sqrt{\frac{D-2}{(D-d)(d-2)}} = \sqrt{\frac{3}{2}} & \text{(Kaluza Klein (KK) tower),} \\ \frac{1}{\sqrt{d-2}} = \frac{1}{\sqrt{2}} & \text{(string tower).} \end{cases} \quad (3)$$

Here D is the dimension before the compactification for the KK tower, and we take $D = d+1$ and $d = 4$. The first one $\lambda_{\text{dc}} = 1$ is just for reference for simplicity. The second one is derived

naturally from the dimension reduction, and it is the same as the case for the KK tower. The third one is the minimum value of λ_{dc} and corresponds to the case where the string tower is the lightest [9–11]. The upper bounds on $\Delta\phi$ as a function of r are illustrated in Fig. 1 for these three cases.

The SDC up to this point provides the upper bounds on the tensor-to-scalar ratio r as a function of the excursion distance of the field $\Delta\phi$. In the next section, we will look at the Lyth Bound, which provides the lower bound on the tensor-to-scalar ratio r as a function of $\Delta\phi$.

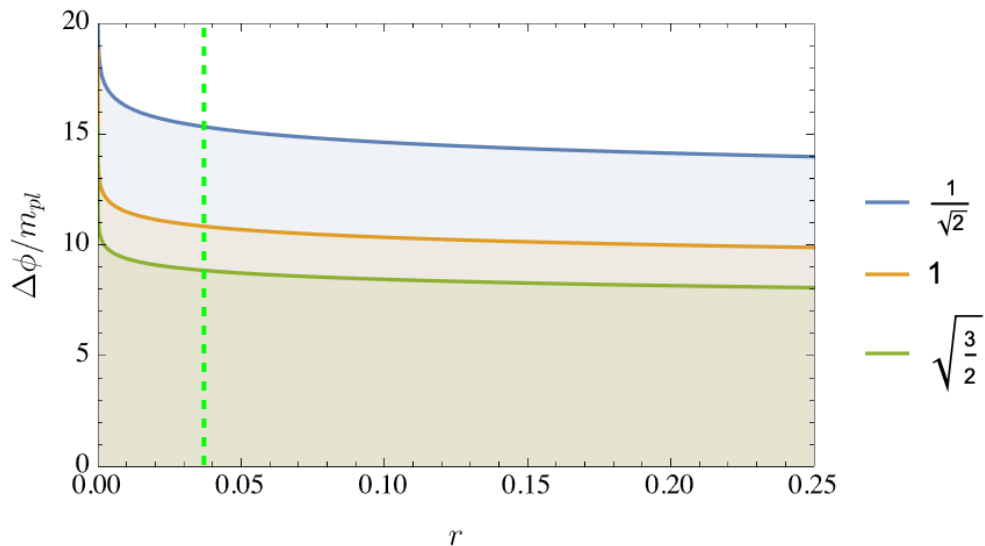


FIG. 1. Upper bounds on the tensor-to-scalar ratio r as a function of the excursion distance of the inflaton $\Delta\phi$. Regarding the reference values for λ_{dc} , we take 1, $\sqrt{\frac{3}{2}}$, and the minimum $\frac{1}{\sqrt{2}}$ in the $d=4$ dimensions. The vertical green dashed line is the observational upper bound on the tensor-to-scalar ratio, $r < 0.036$ (95% C.L.) by the observational data of the Cosmic Microwave Background (CMB) [2, 3].

III. LYTH BOUND

In this section, we consider possible constraints imposed on the model parameters of the inflation by the Lyth Bound. We discuss typical large-field models of the slowroll inflation in which the inflation is induced by the inflaton field slowly-rolling on a flat potential in the beginning. In this case, the inflation ends by the breakdown of the conditions for the

slowroll at a late time due to the fast-rolling on the potential which becomes steeper than the one in the beginning. Then, the Lyth Bound gives an upper bound on the tensor-to-scalar ratio r as a function of the field excursion $\Delta\phi$. Here, we define the first and second slowroll parameters as a function of ϕ as follows.

$$\epsilon(\phi) \equiv \frac{m_{\text{pl}}^2}{2} \left(\frac{V_{,\phi}}{V} \right)^2, \quad (4)$$

$$\eta(\phi) \equiv m_{\text{pl}}^2 \left(\frac{V_{,\phi\phi}}{V} \right)^2. \quad (5)$$

where the subscript $_{,\phi}$ denotes the differentiation with respect to ϕ . The e -folding number during the inflation is defined by

$$N(t) \equiv \ln \frac{a_{\text{end}}}{a(t)} = \int_{a(t)}^{a_{\text{end}}} \frac{da}{a} = \int_t^{t_{\text{end}}} H dt, \quad (6)$$

where the subscript *end* represents the value at the end of the inflation $t = t_{\text{end}}$.

To solve both the horizon problem and the flatness problem, the e -folding number $N(t_{\text{CMB}})$ between a kind of the initial time $t = t_{\text{CMB}}$ ¹, and the end of inflation ($t = t_{\text{end}}$) must be greater than 47 – 62. The upper limit ($N=62$) comes from the upper bound on the energy scale of the potential of the inflation $V^{1/4} \lesssim 10^{16}$ GeV, which corresponds to the upper bound on the tensor-to-scalar ratio $r < 0.036$ [2, 3]. On the other hand, the lower limit ($N = 47$) comes from the most conservative lower bound on the reheating temperature after inflation ($T_R > 4$ MeV [12]). This is obtained from the conditions for the successful big-bang nucleosynthesis in terms of the thermalization of background neutrino and keeping the neutron to proton ratio (n/p) unchanged even by the scatterings of the emitted high-energy particles off the background particles [12–17].

Furthermore, expressing this relation as a function of the scalar field ϕ , we have

$$N(\phi_{\text{CMB}}) = \int_{\phi_{\text{end}}}^{\phi_{\text{CMB}}} \frac{V}{V_{,\phi}} \frac{d\phi}{M_{\text{pl}}^2}. \quad (7)$$

By the definition, the tensor-to-scalar ratio r is also expressed by

$$r \equiv \frac{P_T}{P_\zeta} = 16\epsilon, \quad (8)$$

¹ Correctly, at $t = t_{\text{CMB}}$, the mode, which produced the fluctuation of the CMB, exited the horizon. This is not the initial time. The actual initial time t_{initial} should be shorter than $t_{\text{initial}} \leq t_{\text{CMB}}$

with $P_T = \frac{2V}{3\pi^2 m_{\text{pl}}^4}$ is the tensor perturbation, and $P_\zeta = \frac{V}{24\pi^2 m_{\text{pl}}^4 \epsilon}$ is the scalar curvature perturbation. Regarding the Lyth Bound, expressing the e -foldings number (7) using the slowroll parameter (4), we obtain

$$N(\phi_{\text{CMB}}) = \int_{\phi_{\text{end}}}^{\phi_{\text{CMB}}} \frac{1}{\sqrt{2\epsilon(\phi)}} \frac{d\phi}{m_{\text{pl}}}. \quad (9)$$

Inside the integrand, if we took an initial value as the representative of each variable, e.g., $\epsilon(\phi) = \epsilon(\phi_{\text{CMB}})$ at the beginning $t = t_{\text{CMB}}$, because of the inequality $\epsilon(\phi_{\text{end}}) > \epsilon(\phi_{\text{CMB}})$, we obtain

$$r \leq 2.2 \times 10^{-3} \left(\frac{\Delta N}{60} \right)^{-2} \left(\frac{\Delta\phi}{m_{\text{pl}}} \right)^2, \quad (10)$$

with $\Delta N = N_{\text{end}} - N_{\text{CMB}}$ and $\Delta\phi = |\phi_{\text{CMB}} - \phi_{\text{end}}|$, respectively. This inequality is called the Lyth Bound. In Fig. 2, we plot the Lyth bound which gives the lower bound on $\Delta\phi$ as a function of r .

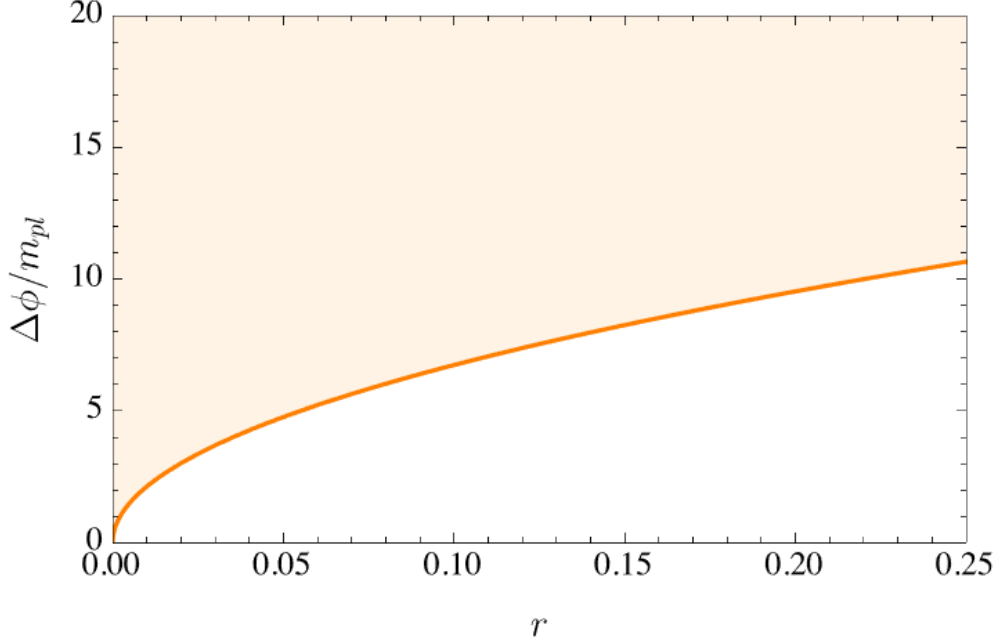


FIG. 2. Lower bound on $\Delta\phi$ as a function of r from the Lyth bound. Here we put $\Delta\phi = 60$ for a representative value in large field models.

IV. INFLATION MODELS

In this section, we discuss the four typical large-field inflation models as follows.

A. Chaotic Inflation

First, we consider the models of Chaotic Inflation [18] which has the simplest potential forms and allows the scalar field to have a very large initial value more than the Planck mass. The potential is represented by the monomial function of ϕ ,

$$V_C(\phi) = V_0 \left(\frac{\phi}{m_{\text{pl}}} \right)^p, \quad (11)$$

where p is an exponent. Then, the tensor-to-scalar ratio r is analytically derived to be

$$r = 8 \left(\frac{\phi}{pm_{\text{pl}}} \right)^{-2}, \quad (12)$$

where ϕ depends on p and N , i.e., $\phi = \phi(p, N)$.

B. Natural Inflation

Next, we discuss the Natural Inflation model [19], which utilizes a pseudo-Nambu-Goldstone boson as the inflaton. The potential of the models of Natural Inflation is given by

$$V_N(\phi) = V_0 \left(1 - \cos \left(\frac{\phi}{F} \right) \right), \quad (13)$$

where F is a parameter (a decay constant) parametrizing the periodicity, and the gentle slope of the potential, which is required for inflation to be naturally realized. Then, the tensor-to-scalar ratio r is expressed by

$$r = 8 \left(\frac{\sin(\phi/F)}{1 - \cos(\phi/F)} \right)^2 \left(\frac{F}{m_{\text{pl}}} \right)^{-2}, \quad (14)$$

where ϕ depends on F and N , i.e., $\phi = \phi(F, N)$.

C. Hilltop Inflation

Concrete forms of the models of Hilltop Inflation were studied by e.g., Refs. [20–25], which describes inflation starting near the top of the hill of the potential. It has been shown that hilltop potentials can be easily obtained from the F-term or the D-term in supersymmetry [20, 21].

The quadratic Hilltop Inflation is parametrized by

$$V_{\text{H}}(\phi) = V_0(1 - \phi^4/\mu_4^4), \quad (15)$$

where μ_4 is a parameter. Then, the tensor-to-scalar ratio r is represented by

$$r = 8 \left(\frac{4m_{\text{pl}}\phi^3}{\mu_4^4 - \phi^4} \right)^2, \quad (16)$$

where ϕ depends on μ_4 and N , i.e., $\phi = \phi(\mu_4, N)$.

D. α attractors

Finally, we discuss the models of α attractors [26, 27]. These models have been proposed and studied in the context of supergravity. For example, the potential for the T -model and E -model of the α attractors is given by

$$V_{\alpha}(\phi) = V_0 \tanh^q \left(\frac{\phi}{\sqrt{6\alpha}m_{\text{pl}}} \right), \quad (17)$$

$$V_{\alpha}(\phi) = V_0 \left(1 - e^{-\sqrt{2}\phi/\sqrt{3\alpha}m_{\text{pl}}} \right)^q, \quad (18)$$

where α is the parameter. α of two models takes the same range as mentioned in the next section, so we use the same representation, α . In this paper, we adopt $q = 2$ for a representative value. By transforming to a canonically normalized field into the Einstein frame, an exponentially flat region is obtained. Then, the tensor-to-scalar ratio of the T -model and E -model is expressed by

$$r = \frac{64}{3\alpha} \left(\sinh \frac{\phi}{\sqrt{6\alpha}m_{\text{pl}}} \cosh \frac{\phi}{\sqrt{6\alpha}m_{\text{pl}}} \right)^{-2}, \quad (19)$$

$$r = \frac{64}{3\alpha} \frac{e^{-2\sqrt{2}\phi/\sqrt{3\alpha}m_{\text{pl}}}}{\left(1 - e^{-\sqrt{2}\phi/\sqrt{3\alpha}m_{\text{pl}}} \right)^2}, \quad (20)$$

where ϕ depends on α and N , i.e., $\phi = \phi(\alpha, N)$.

V. COMBINED LIMITS FROM SWAMPLAND DISTANCE CONJECTURE AND LYTH BOUND

In this section, we consider the region enclosed by the Swampland Distance Conjecture in (2) and the Lyth Bound in (10) in the 2D-plane of the field distance $\Delta\phi$ and the tensor-to-scalar ratio r . Among the representative four inflation models described in Section IV,

we showed the relationship between the field distance and the tensor-to-scalar ratio which are related each other through the e -foldings number N given in Eq. (9). We plot the value of r as a function of $\Delta\phi$ predicted in each model on the same plane and compare it with the region enclosed by the Swampland Distance Conjecture and the Lyth Bound. Here, the parameters adopted in this analysis are shown in Table I. which refers to the ranges of the parameters studied in the paper of the Planck collaboration in 2018 [28].

The results are shown in Fig. 3. The parameter λ_{dc} of the Swampland Distance Conjecture is taken to be 1. For some values within the parameter range of each inflation model, the number of e -foldings is taken from 47 to 62. For example, $p = 1$ for the Chaotic inflation model is the darkest red line plotted traversing the orange Chaotic region in Fig. 3. This red line is obtained by fixing the parameter $p = 1$ and plotting the e -foldings number from 47 to 62. The region obtained when the parameter p is varied within the range of Table I is the region enclosed by the light orange color. The two longest orange curves are obtained by fixing the e -foldings number to be 62 (upper one) or 47 (lower one), respectively, and varying the parameter p . Similarly, the plot for Natural Inflation is the black region enclosed by the black curves. The plot for Hilltop Inflation is the green region enclosed by the green curves. The plot for the α attractor is the light blue region enclosed by the light blue curves. The regions of the T -model and E -model are plotted on extremely close area, so we combined these as the figure of the α attractor. As is clear from the figure, the Natural Inflation model and the α attractor inflation model coincide with the case of $p = 2$ for the chaotic inflation model in the large parameter regions of F/m_{pl} and α , respectively. Similarly, it can be seen that Hilltop inflation in the large parameter region of μ also coincides with the chaotic inflation model of $p = 4/3$ [22].

In Fig. 4, we chose $\lambda_{\text{dc}} = 1/\sqrt{2}$, which is the case for the tower of moduli space. On the

TABLE I. Parameter ranges for each inflation model.

Inflation Model	Parameter Range
Chaotic	$0 < p < 4$
Natural	$0.3 < \log_{10} (F/m_{\text{pl}}) < 2.5$
Hilltop	$-2 < \log_{10} (\mu_4/m_{\text{pl}}) < 2$
α attractor	$-2 < \log_{10} (\alpha) < 4,$

other hand, in Fig. 5, the case of $\lambda_{\text{dc}} = \sqrt{3/2}$, which corresponds to the case of the KK tower.

It is interesting that the case for $\lambda_{\text{dc}} = \sqrt{3/2}$ gives the most stringent upper bounds on r

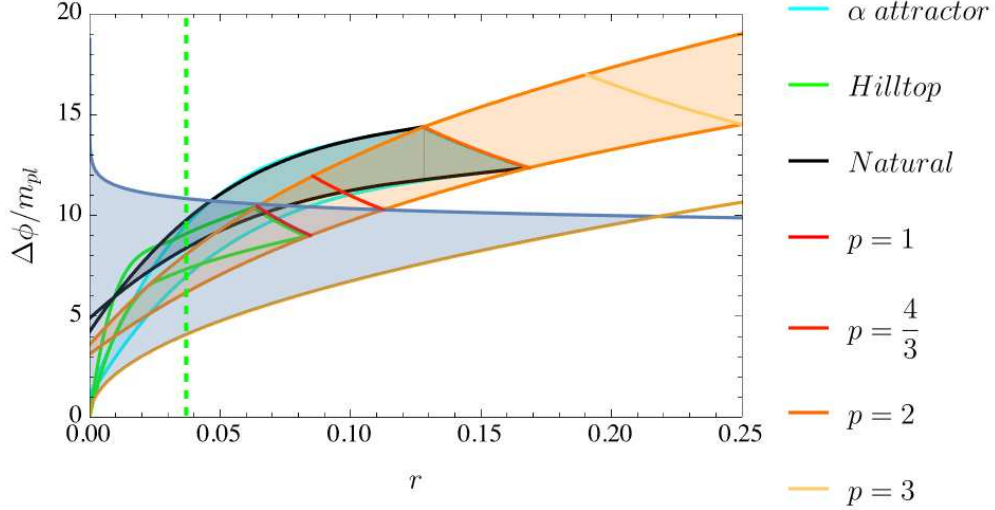


FIG. 3. Allowed regions for four inflation models enclosed by the Swampland Distance Conjecture (blue) and the Lyth Bound (brown). We adopted the parameter $\lambda_{\text{dc}} = 1$ for the Swampland Distance Conjecture. For the theoretical calculations, we plotted the cases for Chaotic inflation with the red lines for $p = 1, 4/3, 2, 3$, Natural inflation (black), Hilltop inflation (green) and α -attractors (cyan). Two lines mean $N=47$ (lower one) and $N=62$ (upper one), respectively. The vertical green dashed line is the observational upper bound on r by the data of the Cosmic Microwave Background (CMB) [2, 3].

and $\Delta\phi$. In this case, it is notable that only the Swampland Distance Conjecture excluded some regions of r at around $r \sim 0.030 - 0.036$ and $\Delta\phi \sim 9 - 10m_{\text{pl}}$, which is stronger than the observational bound from the CMB by the Planck collaboration 2018, $r < 0.036$ (the vertical green dashed line) [2, 3]. Only by such a theoretical requirement, the models of the inflation such as the Natural inflation, the Hilltop inflation and the α -attractors were killed by the Swampland Distance Conjecture (Fig. 5).

Finally, in Fig. 6, we plot the zoom-in figure of the Hilltop inflation models for smaller $\Delta\phi \ll m_{\text{pl}}$ and smaller $r \ll 10^{-3}$. Two curves are plotted for $N=47$ (lower one) and $N=62$ (upper one), respectively. As shown in this figure, the Lyth Bound (orange line) does not work for the Hilltop inflation models in the small r region, ranging from 10^{-12} to 10^{-3} , corresponding to μ_4 between 0.024 and 4.93. The Lyth bound would be a good

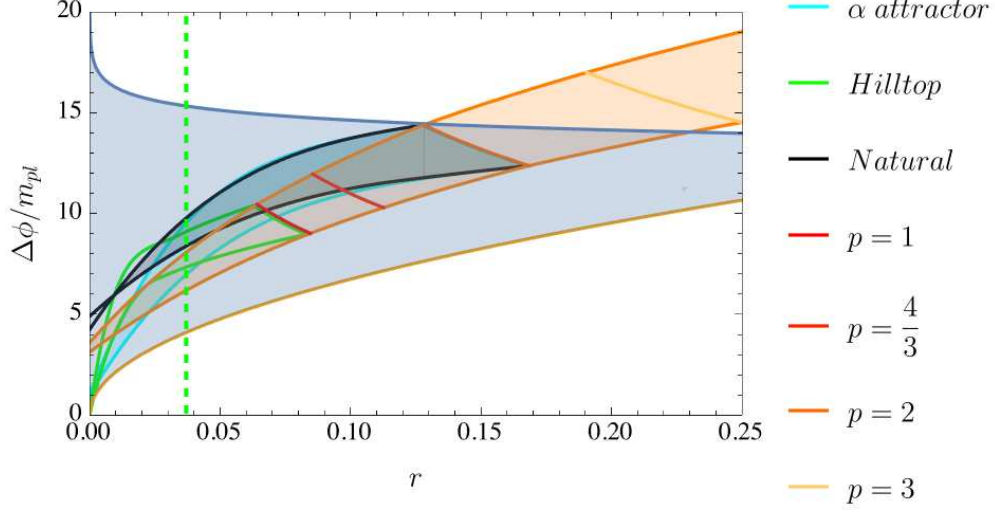


FIG. 4. The same as that of Fig. 3, but for $\lambda_{\text{dc}} = \sqrt{\frac{1}{2}}$.

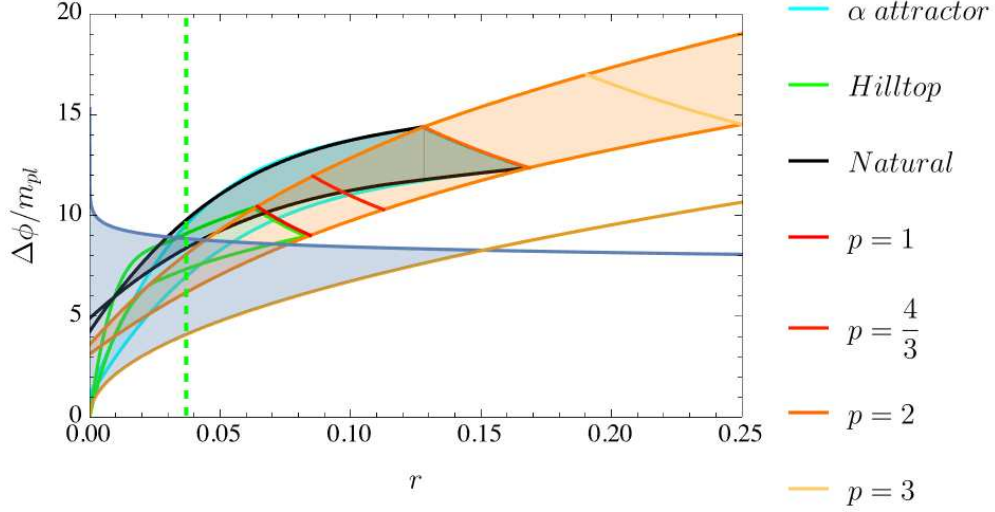


FIG. 5. The same as that of Fig. 3, but for $\lambda_{\text{dc}} = \sqrt{3/2}$.

rough guide for observing the general behavior of the prediction of r in inflation models. However, it sometimes gives a wrong prediction. The results of this study clearly show that when comparing with observed values, it is necessary to calculate the concrete predictions for each model, not just by using the Lyth bound.

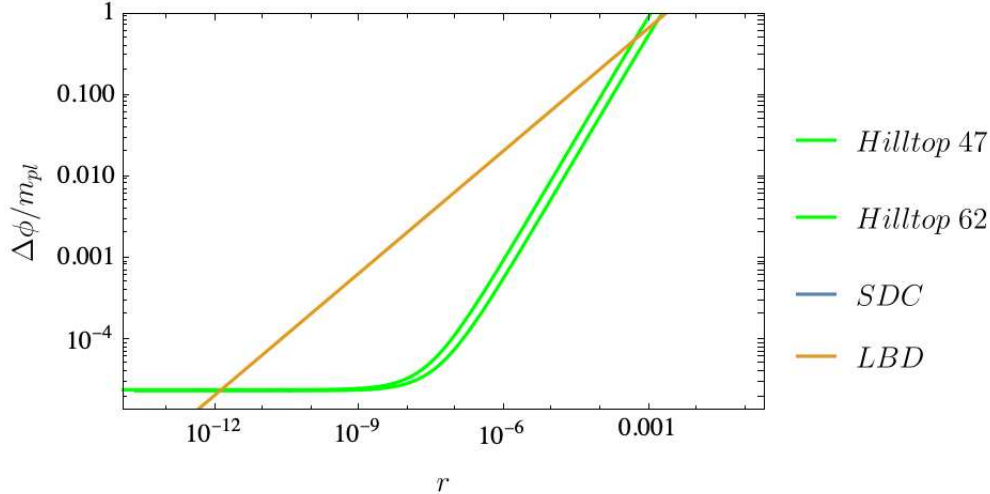


FIG. 6. Zoom-in figure for the Hilltop inflation models (green solid lines) in the $(r, \Delta\phi)$ plane. Two curves are plotted for $N=47$ (upper one) and $N=62$ (lower one), respectively. The orange line represents the Lyth Bound.

VI. CONCLUSIONS

In this paper, we have studied the Swampland conjecture, which has been obtained in the construction of quantum gravity theory, to address the question of how much we can narrow down the large field inflation models to those that are quantum gravity-theoretically advantageous. Among the Swampland conjectures, the property known as the Swampland Distance Conjecture provides an upper bound on the primary gravitational waves produced by large field inflation models. On the other hand, the Lyth bound, which provides a lower bound on primary gravitational waves, plays a complementary role to the Swampland Distance Conjecture. In this paper, we report the following new points for the first time:

In terms of the upper bound on gravitational waves, some of the major large field inflation models are more strongly constrained by the Swampland Distance Conjecture than that of the CMB constraints. It is interesting that the case for $\lambda_{\text{dc}} = \sqrt{3/2}$ gives the most stringent upper bounds on r as a function of $\Delta\phi$. In this case, it is notable that the Swampland Distance Conjecture alone excluded r at around $r \sim 0.030 - 0.036$ and $\Delta\phi \sim 9 - 10m_{\text{pl}}$, which is stronger than the observational bound from the CMB by the Planck collaboration 2018, $r < 0.036$ [2, 3]. Only by such a theoretical requirement, some parameters in the models of the inflation, such as Natural inflation, the Hilltop inflation or the α -attractors

are excluded by the Swampland Distance Conjecture.

We also have found the model parameters that violate the Lyth bound for certain parameter regions of the Hilltop inflation model. Actually the Lyth Bound cannot satisfy the parameters of the Hilltop inflation models in the small r region, ranging from 10^{-12} to 10^{-3} , corresponding to μ_4 between 0.024 and 4.93. When we compare the predictions by a model of the inflation with the observed values, our results clearly show that we have to calculate the concrete predictions for each model, not just by using the Lyth bound.

The latest results from the Atacama Cosmology Telescope (ACT)[29, 30] show a slightly larger spectral index compared to Planck 2018. At the CMB pivot scale $k_{\text{CMB}}=0.05\text{Mpc}^{-1}$, the spectral index was constrained to be $n_s = 0.974 \pm 0.003$ (68% C.L.). This result excludes the Natural inflation model at more than the 2σ level. Furthermore, although the α -attractor model showed good agreement with Planck 2018 regarding the tensor-to-scalar ratio and spectral index, the ACT partially allowed for the e -foldings number $N \gtrsim 57$. Many other parameter regions are under tension at the 2σ level.

In contrast, even though the Hilltop inflation model is excluded for small parameter μ_4 regions, i.e., $\mu_4/m_{pl} \lesssim 14$, the Chaotic inflation model and the Hilltop inflation model are allowed over large regions according to these new results, compared to the previous two models. In particular, the shift towards a larger spectral index by the latest ACT has opened up parameter regions where the parameter p of the Chaotic inflation model is less than one. Interestingly, our results are able to constrain the region where $p < 1$, as shown in Figure 5. This means that the ACT and our results are complementary to each other.

ACKNOWLEDGMENT

This work was in part supported by JSPS KAKENHI Grants Nos. JP24H00976 (Y.H.), JP24K07035 (Y.H.), JP24KF0167 (Y.H.) 23KF0289 (K.K.), No. JP24K07027 (K.K.), and MEXT KAKENHI Grants No. JP24H01825 (K.K.).

-
- [1] J. Ellis and D. Wands, Inflation (2023), (2023), [arXiv:2312.13238 \[astro-ph.CO\]](#).
 - [2] P. A. R. Ade *et al.* (BICEP, Keck), Improved Constraints on Primordial Gravitational Waves using Planck, WMAP, and BICEP/Keck Observations through the 2018 Observing Season,

- [Phys. Rev. Lett. **127**, 151301 \(2021\)](#), [arXiv:2110.00483 \[astro-ph.CO\]](#).
- [3] M. Tristram *et al.*, Improved limits on the tensor-to-scalar ratio using BICEP and Planck data, [Phys. Rev. D **105**, 083524 \(2022\)](#), [arXiv:2112.07961 \[astro-ph.CO\]](#).
 - [4] C. Vafa, The String landscape and the swampland, (2005), [arXiv:hep-th/0509212](#).
 - [5] H. Ooguri and C. Vafa, On the Geometry of the String Landscape and the Swampland, [Nucl. Phys. B **766**, 21 \(2007\)](#), [arXiv:hep-th/0605264](#).
 - [6] M. Scalisi and I. Valenzuela, Swampland distance conjecture, inflation and α -attractors, [JHEP **08**, 160](#), [arXiv:1812.07558 \[hep-th\]](#).
 - [7] N. Aghanim *et al.* (Planck), Planck 2018 results. VI. Cosmological parameters, [Astron. Astrophys. **641**, A6 \(2020\)](#), [Erratum: [Astron. Astrophys. 652, C4 \(2021\)](#)], [arXiv:1807.06209 \[astro-ph.CO\]](#).
 - [8] S.-J. Lee, W. Lerche, and T. Weigand, Emergent strings from infinite distance limits, [JHEP **02**, 190](#), [arXiv:1910.01135 \[hep-th\]](#).
 - [9] M. Etheredge, B. Heidenreich, S. Kaya, Y. Qiu, and T. Rudelius, Sharpening the Distance Conjecture in diverse dimensions, [JHEP **12**, 114](#), [arXiv:2206.04063 \[hep-th\]](#).
 - [10] B. Heidenreich, M. Reece, and T. Rudelius, Repulsive Forces and the Weak Gravity Conjecture, [JHEP **10**, 055](#), [arXiv:1906.02206 \[hep-th\]](#).
 - [11] N. B. Agmon, A. Bedroya, M. J. Kang, and C. Vafa, Lectures on the string landscape and the Swampland, (2022), [arXiv:2212.06187 \[hep-th\]](#).
 - [12] T. Hasegawa, N. Hiroshima, K. Kohri, R. S. L. Hansen, T. Tram, and S. Hannestad, MeV-scale reheating temperature and thermalization of oscillating neutrinos by radiative and hadronic decays of massive particles, [JCAP **12**, 012](#), [arXiv:1908.10189 \[hep-ph\]](#).
 - [13] M. Kawasaki, K. Kohri, and N. Sugiyama, Cosmological constraints on late time entropy production, [Phys. Rev. Lett. **82**, 4168 \(1999\)](#), [arXiv:astro-ph/9811437](#).
 - [14] M. Kawasaki, K. Kohri, and N. Sugiyama, MeV scale reheating temperature and thermalization of neutrino background, [Phys. Rev. D **62**, 023506 \(2000\)](#), [arXiv:astro-ph/0002127](#).
 - [15] S. Hannestad, What is the lowest possible reheating temperature?, [Phys. Rev. D **70**, 043506 \(2004\)](#), [arXiv:astro-ph/0403291](#).
 - [16] K. Ichikawa, M. Kawasaki, and F. Takahashi, The Oscillation effects on thermalization of the neutrinos in the Universe with low reheating temperature, [Phys. Rev. D **72**, 043522 \(2005\)](#), [arXiv:astro-ph/0505395](#).

- [17] P. F. de Salas, M. Lattanzi, G. Mangano, G. Miele, S. Pastor, and O. Pisanti, Bounds on very low reheating scenarios after Planck, [*Phys. Rev. D* **92**, 123534 \(2015\)](#), [arXiv:1511.00672 \[astro-ph.CO\]](#).
- [18] A. Linde, Chaotic inflation, [*Physics Letters B* **129**, 177 \(1983\)](#).
- [19] F. C. Adams, J. R. Bond, K. Freese, J. A. Frieman, and A. V. Olinto, Natural inflation: Particle physics models, power law spectra for large scale structure, and constraints from COBE, [*Phys. Rev. D* **47**, 426 \(1993\)](#), [arXiv:hep-ph/9207245](#).
- [20] L. Boubekur and D. H. Lyth, Hilltop inflation, [*JCAP* **07**, 010](#), [arXiv:hep-ph/0502047](#).
- [21] K. Kohri, C.-M. Lin, and D. H. Lyth, More hilltop inflation models, [*JCAP* **12**, 004](#), [arXiv:0707.3826 \[hep-ph\]](#).
- [22] K. Kohri, C. S. Lim, and C.-M. Lin, Distinguishing between Extra Natural Inflation and Natural Inflation after BICEP2, [*JCAP* **08**, 001](#), [arXiv:1405.0772 \[hep-ph\]](#).
- [23] C.-M. Lin, Type I Hilltop Inflation and the Refined Swampland Criteria, [*Phys. Rev. D* **99**, 023519 \(2019\)](#), [arXiv:1810.11992 \[astro-ph.CO\]](#).
- [24] C.-M. Lin, Topological Eternal Hilltop Inflation and the Swampland Criteria, [*JCAP* **06**, 015](#), [arXiv:1912.00749 \[hep-th\]](#).
- [25] K. Dimopoulos, An analytic treatment of quartic hilltop inflation, [*Phys. Lett. B* **809**, 135688 \(2020\)](#), [arXiv:2006.06029 \[hep-ph\]](#).
- [26] S. Ferrara, R. Kallosh, A. Linde, and M. Porrati, Higher Order Corrections in Minimal Supergravity Models of Inflation, [*JCAP* **11**, 046](#), [arXiv:1309.1085 \[hep-th\]](#).
- [27] R. Kallosh and A. Linde, Non-minimal Inflationary Attractors, [*JCAP* **10**, 033](#), [arXiv:1307.7938 \[hep-th\]](#).
- [28] Y. Akrami *et al.* (Planck), Planck 2018 results. X. Constraints on inflation, [*Astron. Astrophys.* **641**, A10 \(2020\)](#), [arXiv:1807.06211 \[astro-ph.CO\]](#).
- [29] T. Louis *et al.* (ACT), The Atacama Cosmology Telescope: DR6 Power Spectra, Likelihoods and Λ CDM Parameters, (2025), [arXiv:2503.14452 \[astro-ph.CO\]](#).
- [30] E. Calabrese *et al.* (ACT), The Atacama Cosmology Telescope: DR6 Constraints on Extended Cosmological Models, (2025), [arXiv:2503.14454 \[astro-ph.CO\]](#).